

Simulation studies of premixed CH₄/air Microcombustion

P.Bala Murali*

*Department of Mechanical Engineering, Thiagarajar College of Engineering, Madurai, TamilNadu- INDIA)

ABSTRACT

A numerical study of CH₄-air premixed combustion in the micro combustors with a five step global mechanism is performed by solving the two dimensional governing equations of continuity, momentum and species, coupled with the energy equation. A reference case is defined as the combustion in a cylindrical tube with 1 mm inlet diameter and length 10 times its inlet diameter with a uniform velocity profile at the inlet plane. Different physical and boundary conditions have been applied in order to investigate their respective effects on the flame temperature. The conditions studied in the current paper include the combustor size, geometry and inlet velocities. Downscaling the combustion chamber and higher velocities led to reduction in residence time which results in lower combustion efficiency causing insufficient heat generation unable to maintain the self-sustained combustion. The effect of variation in inlet velocity has role in the determining the flame position in combination with given thermal conditions. The results of this paper indicate that these various boundary and physical conditions have effects on the flame temperature to different extent and should be carefully monitored when applied for different applications.

Keywords: Micro combustion, CH₄-air mixture, premixed flame, flame temperature, K-e model

NOMENCLATURE

Ak -- pre-exponential factor of reaction rate (consistent unit)
d-- Inner diameter (m)
D-- Diffusion coefficient (m²/s)
Di-- diffusion coefficient of the *i*-th species (m²/s)
Ek -- activation energy for the *i*-th reaction (J/ (kg mol))
h-- Enthalpy (J/kg)
hconv--convective heat loss coefficient (non-insulated wall) (W/ (m²K))
hi-- enthalpy of the *i*th species (J/kg)
hrad --radiative heat loss coefficient (non-insulated wall) (W/ (m²K))
H-- Spacing between the parallel plates (m)
k-- Thermal conductivity of gas (W/ (mK))
kB--Boltzmann constant (1.380662×10⁻²³ J/K)
L-- Combustor length (m)
P --Pressure (Pa)
q-- Volumetric heat generation rate (W/m³)
qw--heat loss from the non-insulated wall (W)
r-- Radial coordinate (m)
Ru-- universal gas constant (8314.41 J/ (kg mol K))
t-- Wall thickness (m)

T-- Temperature (K)
T0-- ambient temperature (K)
Tu-- temperature of unburned mixture (K)
Tw -- wall temperature at the interface (K)
Two -- temperature of the non-insulated wall (K)
u-- *x* velocity (m/s)
u0-- incoming flow velocity (m/s)
Ui--*x* velocity of the *i*th species (m/s)
V--*y*velocity (m/s)
Vi-- *y* velocity of the *i*th species (m/s)
x-- *x*coordinate (m)
y -- Coordinate for 2D parallel plates (m)
Yi --mass fraction of the *i*th species (kg/kg)

Greek symbols

βk--temperature exponent of the *i*th reaction
□-- Density of the mixture (kg/m³)
□-- Wall emissivity
□-- fuel-air equivalence ratio
□-- Stefan-Boltzmann constant (5.67×10⁻⁸ W/ (m² K⁴))
μ-- Dynamic viscosity (N s/m²)
□*i*--production rate of the *i*th species (kmol/(m³ s))

I. INTRODUCTION

The last few years have experienced a growing trend in the miniaturization of mechanical and electromechanical engineering devices as a result of the progress made in micro-fabrication techniques. The interest in producing miniaturized mechanical

devices opens exciting opportunities in the field of micro-power generation. MEMS-based power generators prototyped, includes the micro gas turbine, the micro-thermoelectric device and the micro-thermo photovoltaic (μ TPV) system. The need to reduce system weight, increase operational life times,

and reduce unit cost has resulted in development of the field of micro-power generation, high-specific energy micro-electromechanical power system. Such work was mainly motivated by the fact that hydrogen and most hydrocarbon fuels represent much higher energy density than the most advanced lithium-ion batteries. The characteristic length of micro combustors using hydrocarbons as fuels may range from several millimetres down to the sub millimetre scale. As a result of the reduced size of the combustors, combustion becomes less efficient due to the intensified heat loss from the flame to the combustor wall, radical destruction at the gas-wall interface and reduced residence time, making the system efficiency relatively low. Essentially, these studies are aimed at achieving a stable combustion in simple geometries such as cylindrical tubes or rectangular channels. The effects and the relationship between thickness and diameter of the tube with the flame propagation were studied in the previous work, and the quenching condition was obtained as a function of the heat-loss parameter [1]. ‘Swiss roll’ combustors (SRC) were simulated to gain insight of micro-scale combustion in prevention of the occurrence of extinction. Increasing wall thermal conductivity (or wall thickness) and emissivity causes the extinction limit to rise [3]. The stability behaviour of single flames stabilized on top of micro tubes indicated that fuels exhibit critical equivalence ratios below which no flame formed, and extinction appeared above certain equivalence ratios [6-17]. The heat exchange through the structure of the micro-combustor can lead to a broadening of the reaction zone. Heat loss to the environment decreases the broadening effect and eventually results in flame quenching [8]. As the combustor length increases, the range of flow conditions for successful ignition becomes smaller [9]. The wall effects such as viscous, cooling and active species destruction shows their prominent effect for decreased diameters of the combustors. In addition, both the volumetric heat loss and the wall shear stress increase with decreasing the diameter [11]. Stable combustion was successfully attained even for mixtures with equivalence ratios outside the conventional flammability limits for methane air mixture with externally heated micro channel [13]. In case of micro flames, the diffusion rate becomes very fast, so that the finite chemical reaction rate starts to govern the phenomenon [14]. In the context of micro combustion, the understanding of flame temperature is necessary to choose the proper material for a micro-combustor.

II. NUMERICAL MODEL

1. Geometry

Figure 1 shows the two - dimensional view of the micro-channel (cylindrical tube and 2D

parallel plates) in which steady-state combustion of a CH₄- air mixture takes place. Symbols d or H represents the diameter of the cylindrical tube or vertical distance between 2D parallel plates, respectively. An assumption is made that the swirl velocity component is zero, meaning a symmetrical flow with respect to the centreline. Thus, the case is simplified to a 2D problem.

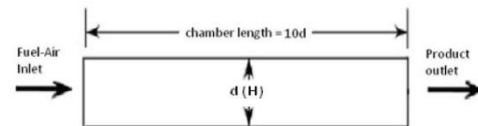


Fig. 1. Schematic of the computational domain with some boundary conditions (not to scale).

2. Governing equations

As the characteristic length of the combustor chamber is still sufficiently larger than the molecular mean-free path of gases flowing through the micro-combustor, fluids can be reasonably considered as continuums and the Navier-Stokes equations are still suitable in the present study. Kuo and Ronny reported that it is more appropriate to predict the combustion characteristics in micro-combustors by using a turbulence model when the Reynolds number is above 500. It is expected that in a micro-combustor, the mixing of various kinds of species is enhanced due to the small space. The turbulence model is better than the laminar model to reflect the enhanced mixing and its effect on combustion characteristics as the main purpose of the micro-combustor fitted with a bluff body is to stabilize the flame under reduced dimensions. Therefore, the realizable k-ε turbulence model is adopted here. The governing equations for the gaseous mixture are shown below:

2.1 Continuity Equation:

$$\frac{\partial}{\partial x}(\rho v_x) + \frac{\partial}{\partial y}(\rho v_y) = 0 \quad \text{--- (1)}$$

2.2 Momentum Equation:

2.2.1 X – Direction:

$$\frac{\partial}{\partial x}(\rho v_x v_x) + \frac{\partial}{\partial y}(\rho v_x v_y) = -\frac{\partial p}{\partial x} + \frac{\partial \tau_{xx}}{\partial x} + \frac{\partial \tau_{xy}}{\partial y} \quad \text{--- (2)}$$

2.2.2 Y – Direction:

$$\frac{\partial}{\partial x}(\rho v_y v_x) + \frac{\partial}{\partial y}(\rho v_y v_y) = -\frac{\partial p}{\partial y} + \frac{\partial \tau_{yx}}{\partial x} + \frac{\partial \tau_{yy}}{\partial y} \quad \text{--- (3)}$$

2.3 Energy:

$$\frac{\partial(\rho v_x h)}{\partial x} + \frac{\partial(\rho v_y h)}{\partial y} = \frac{\partial(k_f \partial T)}{\partial x^2} + \frac{\partial(\rho v_x h)}{\partial y^2} + \sum_i \left[\frac{\partial(h_i \rho D_i \frac{m \partial Y_i}{\partial x})}{\partial x} + \frac{\partial(h_i \rho D_i \frac{m \partial Y_i}{\partial y})}{\partial y} \right] + \sum_i h_i R_i \quad \text{--- (4)}$$

2.4 Species:

$$\frac{\partial(\rho Y_{ivx})}{\partial x} + \frac{\partial(\rho Y_{ivy})}{\partial y} = - \left[\frac{\partial(\rho D_{i,m} \frac{\partial Y_i}{\partial x})}{\partial x} + \frac{\partial(\rho D_{i,m} \frac{\partial Y_i}{\partial y})}{\partial y} \right] \quad \text{--- (5)}$$

As has been shown by many researches that heat conduction in the solid phase exerts an important effect on the combustion, it is necessary to consider the heat transfer in combustor walls in the computation. The energy equation for the solid phase is given as:

$$\frac{\partial y (ks \partial T)}{\partial x^2} + \frac{\partial y (ks \partial T)}{\partial y^2} = 0 \quad \text{--- (6)}$$

Where ks is the thermal conductivity of the wall.

3. Computation scheme

Because CH₄ has much higher burning velocity than other hydrocarbon fuels, it is selected as the fuel in the present study. Because of burning temperature of cH₄ /air mixtures, lean mixtures with equivalence ratios of 0.4, 0.6 and 0.8 and a stoichiometric mixture of equivalence ratio 1 are used to control the maximal temperature. The equivalence ratio ϕ , is a commonly used index to indicate quantitatively whether the fuel-air mixture for a chemical reaction is

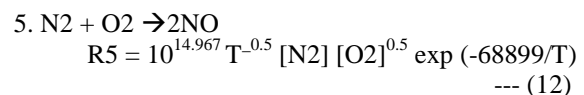
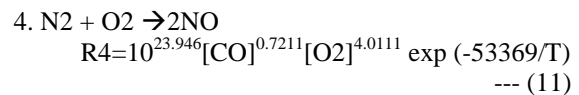
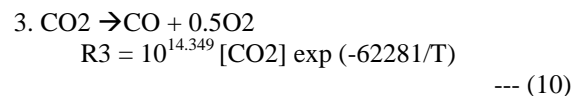
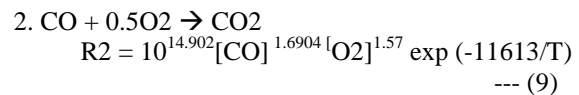
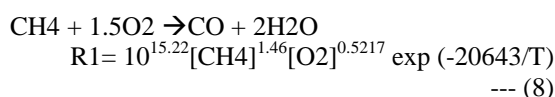
Rich ($\phi > 1$), Lean ($\phi < 1$), or Stoichiometric ($\phi = 1$).

The equivalence ratio is defined as

$$\phi = \frac{\left(\frac{F}{A}\right)}{\left(\frac{F}{A}\right)_{stoi}} \quad \text{--- (7)}$$

where (F/A) and (F/A) stoic are the real and stoichiometric mass ratios of the fuel (F) to the air (A).

To save the computational time only half of the combustor volume is considered. In addition, the following assumptions are made: 1. No work done by pressure and viscous forces; 2. Steady-state. With these assumptions, the Fluent 6.3 solves the governing equations of continuity, momentum, species and energy in the gas phase (for the cylindrical micro-combustor). The 5-step global mechanism used in [5] for CH₄-air reaction is given as below:



The skeletal mechanism (shown above) for methane oxidation (7 species and 5 reactions) is employed in the present study. Its application in the simulation of combustion was found able to yield reasonable results. Based on the above governing equations, the 2D simulations are performed. The governing equations are discretized using the finite-volume method and solved by Fluent Release 6.3. A second order upwind scheme is used to discretize the governing equations and SIMPLE algorithm is used to deal with the pressure velocity coupling. The equations are solved implicitly with a 2D pressure based solver using an under-relaxation method. The solver first solves the momentum equations, then the continuity equation, followed by the updating of the pressure and mass flow rates. The energy and species equations are subsequently solved. Iterations are monitored and checked until a converged solution is obtained. The convergence criteria for the scaled residuals are set to be 1×10^{-6} for continuity, velocity, and energy and for species concentration. The gas density is calculated using the ideal gas law. The gas viscosity, specific heat and thermal conductivity are calculated as a mass fraction-weighted average of all species. The specific heat of each species is calculated using a piecewise polynomial fit of temperature. Numerical convergence is generally difficult because of the inherent stiffness of the matrix (chemistry). For most cases, it was found that energy (temperature) is the last parameter to get converged. The wall thermal conductivity (*k*) is taken to be 20 W/ (mK) (a typical value for stainless steel). The wall has a thickness (*t*) of 0.2 mm and the combustor length (*L*) is 10 times its inlet diameter (*d* or *H*). At the inlet plane, the mixture enters the combustor with a uniform temperature *Tu*= 300 K. At the outlet boundary, the far-field pressure condition is specified. Heat losses from the non-insulated wall to the ambient are given by

$$q_w = h_{conv} (T_{wo} - T_o) + \epsilon \sigma (T_{wo}^4 - T_o^4) \quad \text{--- (13)}$$

where the convective heat transfer coefficient h_{conv} and the wall emissivity ϵ are taken to be 50 W/(m²K) and 0.2 (polished surface without serious oxidation), respectively. In the gas phase, the mesh density was finalized to be 280 grids and 80 grids in the axial direction and radial direction, respectively. A high temperature (~1600 K) is imposed on the entire computational domain as an initial guess for the numerical iteration. It is important to use a temperature high enough to ignite the mixture.

Lower temperature may fail ignition for some cases. The physical and boundary conditions summarized above are applied to all cases in this study. Other conditions may vary from case to case for the purpose of comparison and will be stated in the respective sections.

III. RESULTS AND DISCUSSION

1. Reference case

A 'reference case' needs to be defined in order to facilitate comparison. The geometry of the reference case is a cylindrical tube with an inner diameter of 1 mm. The boundary conditions are summarized as follows:

The boundary conditions are summarized as follows:

- *Inlet* ($x = 0$): $T_u = 300$ K, $u_0 = 0.3, 0.5, 0.8, 1$ m/s, $Y_{CH_4} = 0.034$, (Y_{O_2} can be derived from $\phi = 0.6$ and the air composition);
- *Centreline* ($r = 0$): $\partial u / \partial r = 0$, $\partial T / \partial r = 0$, $\partial Y_i / \partial r = 0$, $v = 0$ (no diffusion flux and zero convective flux across the symmetry plane);
- *Gas-solid interface* ($r = r_0$): $u = 0$, $v = 0$ (nonslip wall), $\partial Y_i / \partial y = 0$ (zero diffusion flux normal to the interface), and the heat flux at the interface is computed using Fourier's law and continuity in temperature and heat flux links the gas and solid phase;
- *Non-insulated wall* ($y = Y_0$):

$$q_w = h_{conv} (T_{wo} - T_o) + \epsilon \sigma (T_{wo}^4 - T_o^4)$$

The above velocity range is used for methane, owing to its lower burning velocity. Based on the simulation results shown in Figure 2, it is noted that as the inlet velocity increases the flame is blown further downstream of the micro-combustor. Higher velocity which implies higher mass flow rate requires longer heating length (by the combustor wall) for the mixture to be heated up to ignition temperature. For $u_0 = 0.3$ m/s, the flame is anchored

near the entrance and the highest temperature of gases lies at the centreline of the combustor. For the velocities 0.5 m/s and above, position of the increased temperature zone of gases shifts from the centreline to the wall. Figure 2 indicates that in the pre-flame zone, the wall temperature is higher than the mixture temperature, suggesting the direction of heat transfer is from the wall to the fuel-air mixture. The high temperature zone of the methane-air flames occupies a wider span of the radial section.

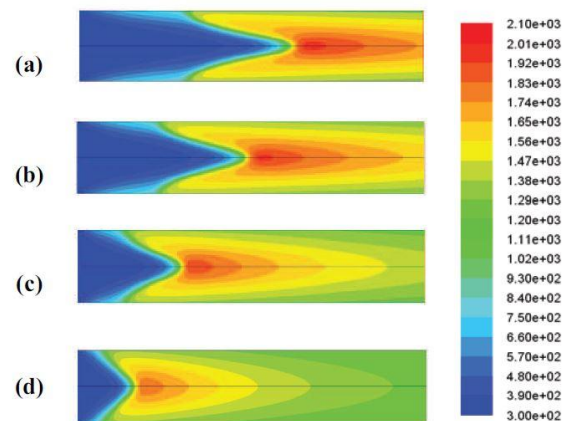


Fig. 2. Contours of temperature with different uniform inlet velocities, cylindrical tube of $d = 1$ mm, (a) $u_0 = 1.0$ m/s (b) $u_0 = 0.8$ m/s (c) $u_0 = 0.5$ m/s (d) $u_0 = 0.3$ m/s.

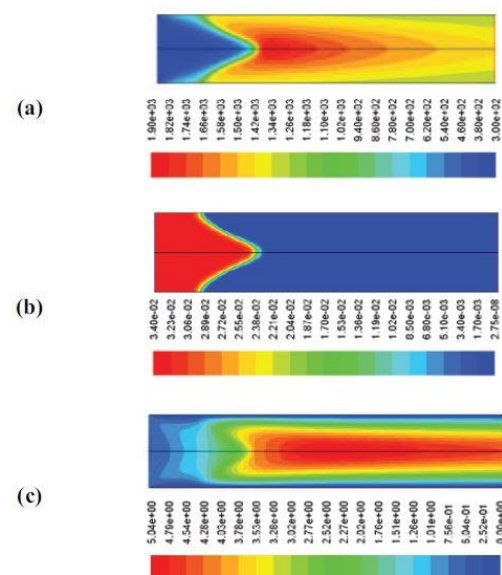


Fig. 3. Contours of (a) temperature, (b) methane mass fraction and (c) axial velocity, $d = 1$ mm, $u_0 = 0.5$ m/s, for gas phase in cylindrical combustion chamber.

Figure 3 shows the contours of temperature, methane mass fraction and axial velocity for the case of $u_0 = 0.5$ m/s. It can be seen that a major part

of methane is consumed within a thin layer of reactions. Axial velocity near the entrance gradually increases in the region upstream of the flame front. But in the region of high temperature the axial velocity is highly accelerated which can be observed along the centreline of the combustion chamber. The normalized temperature profiles in the radial direction for the case of $u_0 = 0.3$ m/s is plotted in Fig. 4. It can be seen from the difference in terms temperature distribution in radial direction that for axial distance 0.75 mm, the mixture is simply heated up to the radial distance of 0.0003 mm. Further, radial distance for that position has decreased value of preheating. For axial distance beyond 1.0 mm exothermic reactions are initiated, indicating high temperature zone.

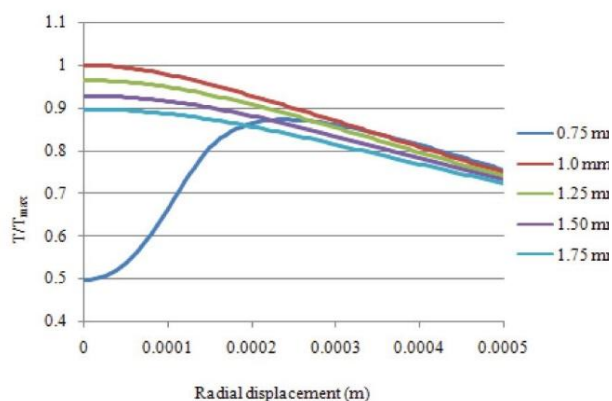


Fig. 4. Normalized temperature profiles, for $d = 1$ mm, $u_0 = 0.3$ m/s.

2. Effect of combustor size and geometry

In order to investigate the effects of combustor size for the methane–air mixture, a larger combustor ($d = 2$ mm) is modelled by keeping the same shape aspect ratio. Other conditions (wall thickness, boundary conditions, etc.) are identical to those for the reference case ($d = 1$ mm). By defining the flame temperature as the highest temperature in the gas phase, the effects of combustor size on the flame temperature for given velocity range are shown in Figure 5.

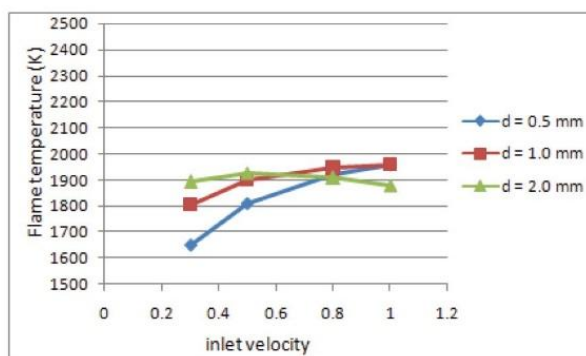


Fig. 5. Effects of combustor size on the flame temperature cylindrical tube.

Lines connecting symbols are only for the sake of visualization. For both combustors of diameters 0.5 mm, and 1 mm, the increase of inlet velocity results in higher flame temperature. However, when the inlet velocity is higher than 0.5 m/s, the smaller combustor ($d = 1$ mm) gives higher flame temperature than the larger one ($d = 2$ mm).

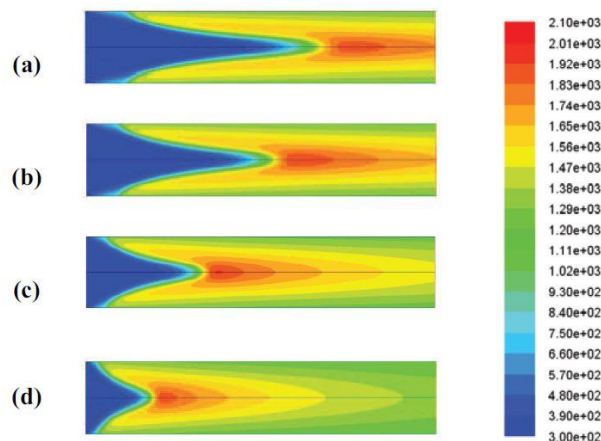


Fig. 6. Contours of temperature with different uniform inlet velocities, cylindrical tube of $d = 2$ mm, (a) $u_0 = 1.0$ m/s (b) $u_0 = 0.8$ m/s (c) $u_0 = 0.5$ m/s (d) $u_0 = 0.3$ m/s.

In order to understand this result, the flame structure needs to be examined. For the $d = 2$ mm combustor, the flame structure shows that the high temperature zone is attached to the combustor wall. The temperature contours for the $d = 2$ mm micro combustor with medium ($u_0 = 0.5$ m/s) and high ($u_0 = 1.0$ m/s) velocities are shown in Figure 6.

Compared to Figure 2 ($d = 1$ mm), the difference in terms of flame structure is obvious. As the combustor diameter is increased from 1 to 2 mm, the radial length for mass diffusion is doubled. As a result, the temperature at the centreline zone of the larger combustor is more controlled by axial convection than radial diffusion. In the region of reaction, heat diffuses in the radial direction to the centreline zone, which accompanied with the lowered flame temperature. In addition, another factor that needs to be considered is that heat recirculation through the combustor wall is more significant in the smaller micro combustor. Apart from the explanations given above, incomplete combustion could also be a possible reason for the lowered flame temperature in the larger combustor ($d = 2$ mm).

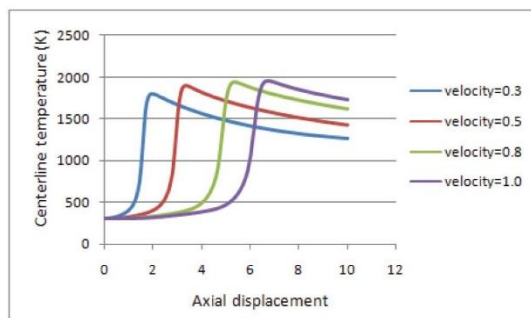


Fig. 7. Centreline temperature profiles for Cylindrical Combustor of $d = 1\text{mm}$

Figure 7 shows the centreline temperature profiles for different flow velocities. It can be seen that as the velocity is increased to 0.8 m/s, the highest centreline temperature approaches to or at the combustor exit, implying that the combustion process could be incomplete. Based on the limited cases simulated in the present study, it is noted that for CH₄-air premixed combustion, when the flow velocity is above a certain level, the conclusion that ‘smaller combustor gives lower flame temperature’ does not hold. The geometry is another important factor for combustor design. Cylindrical tubes and rectangular channels are the two commonly used geometries. For simplicity, a model of 2D parallel plates is employed to represent the rectangular channels. In the simulation, the spacing (H) between the plates is taken to be 1 mm, same as the inner diameter in the reference case. Thus, the hydrodynamic diameter ($= 2H$) of the 2D case is twice that of the cylindrical tube ($d = 1\text{mm}$). Other physical and boundary conditions remain unchanged from the reference case. A theoretical analysis showed that the quenching distance for the parallel plates is related to that for the cylindrical tube by a factor of 0.65. In other words, when $H = 0.65d$, the heat loss condition of a cylindrical tube is identical to a 2D planar channel. The 2D case with the spacing of $H = 1\text{mm}$ is modelled for comparison. The variation of exit temperature with the flow velocity for the two cases is plotted in Figure 8.

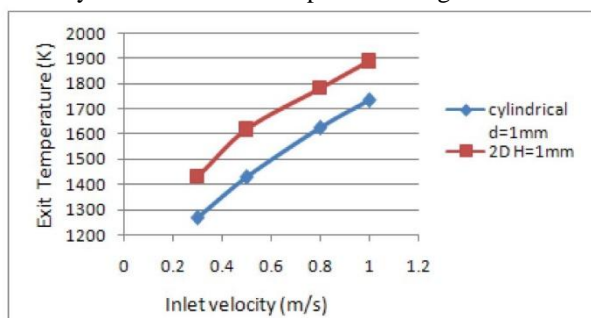


Fig. 8. Effect of combustor geometry on the flame temperature.

Lines connecting symbols are only for the sake of visualization. From Figure 8, it can be seen that the $H = 1\text{mm}$ case has higher exit temperature than the $d = 1\text{mm}$ case over the given velocity range, owing to the difference in the hydrodynamic diameter. Similar observations obtained for the comparison between $H = 2\text{mm}$ and $d = 2\text{mm}$. Other than the factors (radial diffusion, heat recirculation and incomplete combustion) discussed above, the difference in terms of heat loss area between the two geometries could be another reason. More in-depth investigation on this result is needed, but it can be concluded at this point that the hydrodynamic diameter alone is not sufficient to correlate the two combustor geometries. This conclusion could be useful when attempting to alter the shape of the micro-combustor without affecting the flame temperature too much. However, it should be noted that in practice, the result may not be strictly valid due to the three-dimensional nature of a rectangular planar channel.

3. Effect of inlet velocity

The temperature contours and profiles obtained for the given uniform velocity range for cylindrical diameter of 1 mm are plotted in Figure 2 and 7 respectively. Similar type of behaviour obtained for the temperature profiles with increased velocities for the other diameters also. The flame position is essentially an overall result of the thermal conditions and the flow field. In the pre-flame zone, the inlet velocity profile may affect the heat transfer from the wall to the unburned mixture, thus affecting the heating length for the ignition to occur. It is hard to predict the flame position due to the close coupling between the thermal (both gases and solid) and flow fields in the micro combustors.

IV. CONCLUSION

Flame temperature is one of the most important parameters to characterize a combustion process. A numerical study of CH₄-air premixed combustion in micro combustors was undertaken by examining the effects of combustor size and geometry, inlet velocities on the flame temperature. A reference case was defined as a premixed CH₄-air combustion in a cylindrical tube ($d = 1\text{mm}$) with a uniform velocity profile at the inlet plane. It was shown that a larger combustor ($d = 2\text{mm}$) gives higher flame temperature only when the flow velocity is below 0.5 m/s, whereas for diameters of 0.5 and 1 mm increase of inlet velocity results in higher flame temperature. Downscaling the combustion chamber and higher velocities led to reduction in residence time which results in lower combustion efficiency causing insufficient heat generation unable to maintain the self-sustained combustion. The effect of variation in inlet velocity

has role in the determining the flame position in combination with given thermal conditions. With regard to the combustor geometry, a 2D planar channel ($H = 1$ mm) represents higher exit temperature than a cylindrical tube with $d = 1$ mm, over the inlet velocity range investigated in the present study. Similar phenomenon was observed for combustor of 2 mm passage. These conclusions could be useful when attempting to alter the shape of micro-combustion chambers with taking into account the effect on the flame temperature to different extent and should be carefully monitored when applied in different applications.

ACKNOWLEDGEMENTS

Dr.P.Maran, Assistant Professor,
Department of Mechanical Engineering, Thiagarajar
college of Engineering , Madurai, Tamil Nadu,
India-625015.

Email:pmmech@tce.edu

PrashanthDevaraj, Mechanical
Engineering, Thiagarajar college of Engineering,
Madurai, Tamil Nadu, India-625015

Email: prashanthdevaraj@ymail.com

REFERENCES

- [1]. Barrios, E., Prince, J.C., and Trevino, C., 2008. The role of duct thickness on the quenching process of premixed flame propagation, *Combustion Theory and Modelling* 12 (1), 115–133.
- [2] Bell, J.B., Day, M.S., Grcar, J.F., and Lijewski, M.J., A Computational Study of Equivalence Ratio Effects in Turbulent, Premixed Methane-Air Flames, *Lawrence Berkeley National Laboratory, Berkeley USA*.
- [3] Chen, M., Buckmaster, J., 2004, Modelling of combustion and heat transfer in 'Swiss roll' micro-scale combustors, *Combust. Theory Modelling*, 8, 701–720.
- [4] Embid, P.F., Majda, A.J., Souganidis, P.E., 1994, Effective Geometric Front Dynamics for Premixed Turbulent Combustion with Separated Velocity Scales, *Combust. Sci. and Tech.*, 103, 85-115.
- [5] Fluent Inc., Fluent Release 6. 3 User Guide, Fluent Inc., 2006.
- [6] Huang, Y., and Yang, V., 2004, Bifurcation of flame structure in a lean premixed swirl stabilized combustor: transition from stable to unstable flame, *Combustion and Flame*, 136, 383–389.
- [7] Kamali, R., Binesh, A.R., Hossainpour, S., 2007, Numerical Simulation of Wall Treatment Effects on the Micro-Scale Combustion, *World Academy of Science, Engineering and Technology*, 35.
- [8] Leach, T.T., Cadou, C.P., and Jackson, G.S., 2006, Effect of structural conduction and heat loss on combustion in micro channels, *Combustion Theory and Modelling*, 10 (1), 85–103.
- [9] Li, J., Chou, S.K., Huang, G., Yang, W.M., Li, Z.W., 2009, Study on premixed combustion in cylindrical micro combustors: Transient flame behaviour and wall heat flux, *Experimental Thermal and Fluid Science*, 33, 764–773.
- [10] Li, J., Chou, S.K., Yang, W.M., Li, Z.W., 2009, A numerical study on premixed micro combustion of CH₄–air mixture: Effects of combustor size, geometry and Boundary conditions on flame temperature, *Chemical Engineering Journal*, 150, 213–222.
- [11] Li, Z.W., Chou, S.K., Shu, C., Xue, H., and Yang, W.M., 2005, Characteristics of premixed flame in micro combustors with different diameters, *Applied Thermal Engineering*, 25, 271–281.
- [12] Lipatnikov, A.N., and Chomiak, J., 1998, Lewis Number Effects in Premixed Turbulent Combustion and Highly Perturbed Laminar Flames, *Combust. Sci. and Tech*, 137, 277– 298.
- [13] Maruta, K., Parc, J.K., Oh, K.C., Fujimori, T., Minaev, S.S., and Fursenko, R.V., 2004, Characteristics of Micro scale Combustion in a Narrow Heated Channel, *Combustion, Explosion, and Shock Waves*, 40 (5), 516–523.
- [14] Nakamura, Y., Yamashita, H. and Saito, K., 2006, A numerical study on extinction behaviour of laminar micro-diffusion flames, *Combustion Theory and Modelling*, 10 (6), 927–938.
- [15] Ronney, P.D., Analysis of non-adiabatic heat recirculating combustors, 2003, *Combustion and Flame*, 135, 421–439.
- [16] Yang, W.M., Chou, S.K., Shu, C., Li, Z.W., Xue, H., 2002, Combustion in micro cylindrical combustors with and without a backward facing step, *Applied Thermal Engineering*, 22, 1777–1787.
- [17] Yuasa, S., Oshimi, K., Nose, H., Tennichi, Y., 2005, Concept and combustion characteristics of ultra-micro combustors with premixed flame, *Proceedings of the Combustion Institute*, 30, 2455–2462.
- [18] Kuo CH, Ronney PD .Numerical modelling of non-adiabatic heat recirculating combustors. *Proc Combust Inst* 2007; 31:32; 77-84